JACS
JOURNAL OF THE AMERICAN CHEMICAL SOCIETY
Communication
pubs.acs.org/JACS

Two-State Reactivity Mechanism of Benzene C−C Activation by Trinuclear Titanium Hydride

Bo Zhu, Wei Guan,* Li-Kai Yan, and Zhong-Min Su*

Institute of Functional Materials Chemistry and Local United Engineering Lab for Power Battery, Faculty of Chemistry, Northeast Normal University, Changchun 130024, P. R. China

Supporting Information

ABSTRACT: The cleavage of inert C−C bonds is a central challenge in modern chemistry. Multinuclear transition metal complexes would be a desirable alternative because of the synergetic effect of multiple metal centers. In this work, carbon−carbon bond cleavage and rearrangement of benzene by a trinuclear titanium hydride were investigated using density functional theory. The reaction occurs via a novel "two-state reactivity" mechanism. The important elementary steps consist of hydride transfer, benzene coordination, dehydrogenation, oxidative addition, hydride−proton exchange, and reductive elimination. Most importantly, the ground-state potential energy surface switches from nearly degenerate triplet and antiferromagnetic singlet states to a closed-shell singlet state in the dearomatization of benzene, which effectively decreases the activation barrier. Furthermore, the roles of the transition metal centers and hydrides were clarified.

The C−C bond is the basis of the organic molecular skeleton. Selective C−C activation is of significant interest because of its fundamental and widespread applications in the petroleum industry, environmental protection, pharmaceuticals, and so forth.[1] In the past decade, several transition metal complexes have been developed to selectively cleave C−C bonds by utilizing relief of ring strain,[2] aromatization,[3] cyclometalation,[4] β-carbon elimination,[5] and cocatalysts.[6] Nevertheless, C−C bond cleavage in some special hydrocarbon compounds still faces tremendous challenges, especially that of arenes with σ bonds and delocalized π electrons between carbon atoms. In comparison with mononuclear transition metal complexes, multinuclear ones have recently attracted much attention in such transformations because of the synergetic effect of multiple metal centers.[7] A particularly interesting example is the cleavage and rearrangement of the quite inert C−C bond of benzene by a trinuclear titanium polyhydride complex, $(Cp'Ti)_3(\mu_3\text{-}H)(\mu\text{-}H)_6$,[8] to afford a 2-methylcyclopentenyl complex,[9] as shown in Scheme 1. In this reaction, the multinuclear titanium hydride could be considered as a unique platform for the C−C bond cleavage of benzene. As far as we know, this is the first example of selective C−C bond activation of aromatic molecules by three cooperating metal centers. Although an intermediate of the reaction process, $(Cp'Ti)_3(C_6H_7)(\mu\text{-}H)_4$, was observed in the experiment,[9] the mechanistic details of the reaction and the roles of the transition metal centers and hydrides in $(Cp'Ti)_3(\mu_3\text{-}H)(\mu\text{-}H)_6$ are still ambiguous. Such theoretical knowledge could help us to understand and further develop inert C−C bond activation reactions.

Scheme 1. Experimentally Reported C−C Bond Cleavage and Rearrangement of Benzene by the Trinuclear Titanium Heptahydride Complex $(Cp'Ti)_3(\mu_3\text{-}H)(\mu\text{-}H)_6$

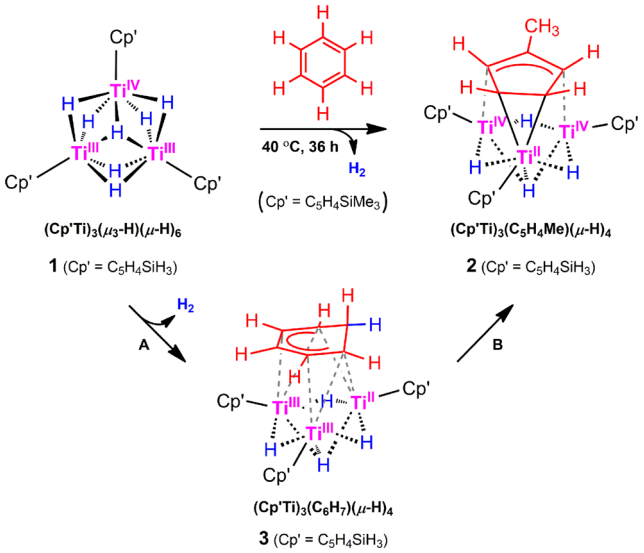

Here we theoretically investigated all of the reaction processes involved in Scheme 1 using model complex **1**, in which the Cp′ group of $(Cp'Ti)_3(\mu_3\text{-}H)(\mu\text{-}H)_6$ was simplified to $C_5H_4SiH_3$, with benzene as the substrate. Geometry optimizations, intrinsic reaction coordinate (IRC) calculations, and vibrational frequency calculations were performed at the (U)B3LYP[10,11]/[6-31G(d)/6-31++G(d,p)(H^-)/SDD(Ti)] level to examine the closed-shell (CS) singlet, antiferromagnetic (AF) singlet, and triplet (T) potential energy surfaces (PESs). Electronic energies were evaluated at the (U)M06[12]-(CPCM[13])/[6-311++G(d,p)/SDD(Ti)] level. These calculations were carried out with the Gaussian 09 program[14] (see the Supporting Information (SI) for computational details). Throughout this paper, the discussion is based on Gibbs energy changes relative to C_6H_6 + antiferromagnetic singlet **1**.

As shown in Scheme 1, the target reaction can be divided into two parts to be discussed. Reaction **A** is the conversion of

Received: March 6, 2016
Published: August 22, 2016

DOI: 10.1021/jacs.6b02433
J. Am. Chem. Soc. 2016, 138, 11069−11072

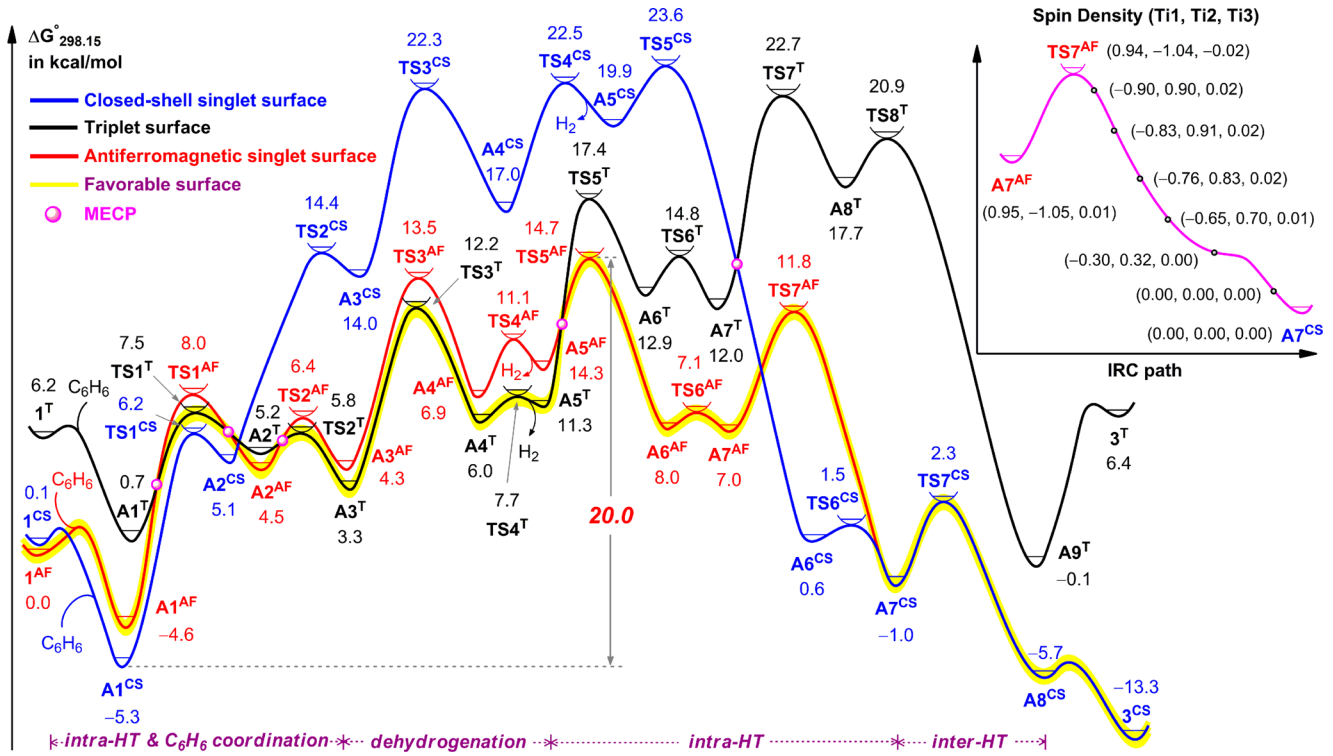

Figure 1. Gibbs energy profiles ($\Delta G^{\circ}_{298.15}$) of reaction **A** in Scheme 1.

1 + C_6H_6 to **3** + H_2. Reaction **B** is the transformation of **3** to methylcyclopentenyl complex **2**.

In comparison with the C_6H_6-free mechanism for reaction **A**, the C_6H_6-coordinated pathway is considered to be more favorable (see Figure S3). This suggests that the C_6H_6 coordination occurs before H_2 dissociation ($+C_6H_6$, then $-H_2$). In the C_6H_6-coordinated mechanism, the H−H bond tends to form prior to the intermolecular hydride transfer (inter-HT) from **1** to C_6H_6 (see Figure S4). The CS singlet, AF singlet, and triplet PESs are described in Figure 1, and optimized structures for selected important stationary points are shown in Figure 2 (see Figures S5−S7 for the whole set of optimized structures). It should be noted that the translational entropy correction causes $\mathbf{A5}^{\mathbf{T}}$ to lie above $\mathbf{TS4}^{\mathbf{T}}$ by 3.6 kcal/mol in this bimolecular process. A similar trend can be seen in the $\mathbf{TS4}^{\mathbf{AF}} \rightarrow \mathbf{A5}^{\mathbf{AF}}$ transformation (see Table S4). In addition, $\mathbf{TS6}^{\mathbf{AF}}$ lies below $\mathbf{A6}^{\mathbf{AF}}$ by 0.9 kcal/mol when the single-point-energy correction is taken into account (see Table S5), suggesting that this step is a low-barrier or even barrier-free transformation. As can be seen in Figure 1, reaction **A** consists of four fundamental processes: (i) intramolecular hydride transfer (intra-HT) and C_6H_6 coordination, (ii) dehydrogenation, (iii) intra-HT, and (iv) inter-HT. The intra-HT after dehydrogenation is the rate-determining step of reaction **A**. The most favorable reaction pathway starts from antiferromagnetic singlet **1** ($\mathbf{1}^{\mathbf{AF}}$) and then proceeds through the nearly degenerate triplet and AF singlet PESs to release H_2. The following intra-HT proceeds in the AF singlet state. The final inter-HT switches to the CS singlet PES to yield the stable intermediate $\mathbf{3}^{\mathbf{CS}}$. Spin inversion between the triplet and AF singlet PESs can be observed and effectively decreases the activation barrier. This spin-crossing phenomenon was termed "two-state reactivity" as a new concept in organometallic chemistry.[15−17] The Gibbs activation energy ($\Delta G^{\circ\ddagger}$) and the Gibbs free energy change (ΔG°) are 20.0 and −13.3 kcal/mol,

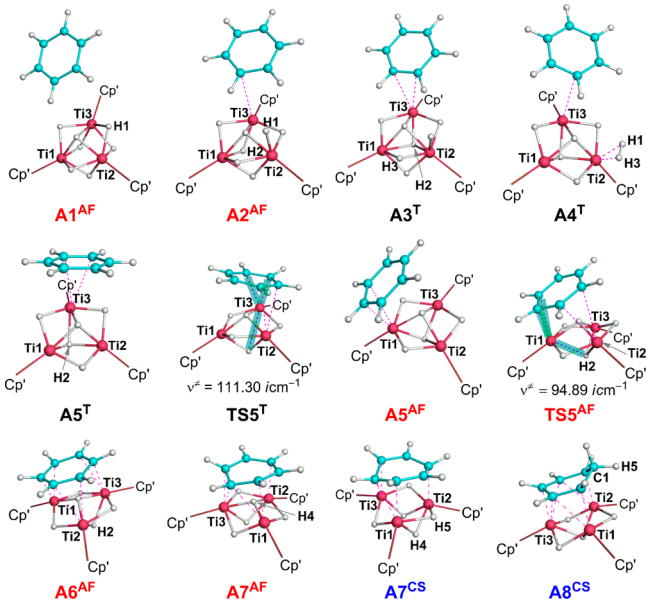

Figure 2. Optimized structures for selected important stationary points in the PESs in Figure 1.

respectively. The energy barrier can be overcome under the experimental conditions.[9]

For complex **1**, DFT and CASPT2/CASSCF calculations showed that the ground state is the AF singlet state (see the SI for CASSCF calculations), which is in reasonable agreement with experimental NMR analyses.[9] Furthermore, the selected important geometrical parameters of $\mathbf{1}^{\mathbf{AF}}$ show the best consistency with experimental measurements (see Table S1).

The exothermic process for the production of $\mathbf{A1}^{\mathbf{AF}}$ arises from the interaction between C_6H_6 and $\mathbf{1}^{\mathbf{AF}}$, which induces a stabilization energy that is much larger than the energy

DOI: 10.1021/jacs.6b02433
J. Am. Chem. Soc. 2016, 138, 11069−11072

destabilization resulting from the entropy decrease. The triplet and AF singlet surfaces cross in the intra-HT and C_6H_6 coordination ($\mathbf{A1}^{AF} \rightarrow \mathbf{A3}^{T}$) because there are similar structures of stationary points in both PESs. These spin inversions alter the most favorable reaction pathway through the minimum-energy crossing points (MECPs). In the $\mathbf{A1}^{AF} \rightarrow \mathbf{A2}^{AF}$ transformation, the μ-H1−Ti3 bond is cleaved and μ-H1 becomes a terminal H coordinated to Ti2 alone. The $\Delta G^{\circ\ddagger}$ and ΔG° values for this step are 12.1 and 9.1 kcal/mol, respectively. It should be noted that the initial intra-HT in the CS singlet PES ($\mathbf{A1}^{CS} \rightarrow \mathbf{A2}^{CS}$) involves a μ_3-H → terminal H rather than a μ-H → terminal H transformation (Figure S5). The difference is attributed to the binding energies of μ-H and μ_3-H with the rest of $\mathbf{1}^{CS}$ and $\mathbf{1}^{T}$, respectively (see Table S6). The calculated results suggest that μ_3-H is active in the CS singlet PES, whereas μ-H is active in the triplet PES. From $\mathbf{A2}^{AF}$, μ-H2 moves toward the center of the trinuclear titanium moiety through the MECP and transition state $\mathbf{TS2}^{T}$ to provide intermediate $\mathbf{A3}^{T}$ with a Ti3···C_6H_6 η^2-coordinate bond. In this step, μ-H2 becomes μ_3-H2 interacting with three titanium atoms. The $\Delta G^{\circ\ddagger}$ and ΔG° values for this step are only 1.3 and −1.2 kcal/mol, respectively.

The dehydrogenation occurs via H−H bond formation and H_2 dissociation. In the former step, a μ-H3 → terminal H3 transformation similar to the above elementary step occurs through $\mathbf{TS3}^{T}$ to afford $\mathbf{A4}^{T}$. The $\Delta G^{\circ\ddagger}$ and ΔG° values for this step are 8.9 and 2.7 kcal/mol, respectively. Next, H_2 dissociation occurs through $\mathbf{TS4}^{T}$ to afford the reduced Ti(III)−Ti(II)−Ti(III) complex $\mathbf{A5}^{T}$. In this step, the H1−H3 group with a covalent bond dissociates from the complex to become a free H_2 molecule. This step has small $\Delta G^{\circ\ddagger}$ and ΔG° values of 1.7 and 5.3 kcal/mol, respectively.

In the second intra-HT ($\mathbf{A5}^{T} \rightarrow \mathbf{A7}^{AF}$), spin inversion between the triplet and AF singlet PESs effectively decreases the activation barrier. The ground-state PES switches from the triplet state to the AF singlet state via an MECP. First, the C_6H_6 moiety of $\mathbf{A5}^{T}$ approaches the trinuclear titanium pentahydride moiety through $\mathbf{TS5}^{AF}$ to afford $\mathbf{A6}^{AF}$. Simultaneously, μ_3-H2 becomes μ-H2 interacting with Ti2 and Ti3. This step has a small $\Delta G^{\circ\ddagger}$ value of 3.4 kcal/mol. Then, further coordination of the C_6H_6 moiety moderately induces deformation of the benzene ring. In this barrier-free $\mathbf{A6}^{AF} \rightarrow \mathbf{A7}^{AF}$ step, μ_3-H4 moves close to the trinuclear titanium plane.

Interestingly, an electronic state transformation (EST) was found prior to the inter-HT. As shown in Figure 1, the transition state $\mathbf{TS7}^{AF}$ is shown to connect the antiferromagnetic singlet $\mathbf{A7}^{AF}$ and the closed-shell singlet $\mathbf{A7}^{CS}$ on the IRC path. In this step, μ_3-H4 moves moderately downward below the trinuclear titanium plane and then becomes μ-H4 interacting with Ti1 and Ti2. The spin densities for six selected points in the forward direction of the IRC path indicate that spin polarization gradually disappears. The closed-shell singlet Ti(III)−Ti(III)−Ti(II) complex $\mathbf{A7}^{CS}$ is finally produced. The EST has a small $\Delta G^{\circ\ddagger}$ value of 4.8 kcal/mol and a negative ΔG° value of −8.0 kcal/mol. In addition, spin inversion between the triplet and CS singlet PESs was also observed through an MECP.[18] However, the $\mathbf{A7}^{T} \rightarrow$ MECP $\rightarrow \mathbf{A6}^{CS}$ pathway is less favorable than the EST pathway. The electronic structures and relative stabilities of $\mathbf{A7}^{T}$, $\mathbf{A7}^{AF}$, and $\mathbf{A6}^{CS}$ were confirmed by CASPT2/CASSCF calculations (see Figure S2 and Tables S7 and S8).

The last stage of reaction **A** proceeds along the CS singlet PES via inter-HT to the C_6H_6 moiety ($\mathbf{A7}^{CS} \rightarrow \mathbf{3}^{CS}$). μ-H5 of $\mathbf{A7}^{CS}$ is anchored toward C1 of the C_6H_6 moiety through $\mathbf{TS7}^{CS}$ to yield $\mathbf{A8}^{CS}$. The $\Delta G^{\circ\ddagger}$ and ΔG° values for this step are 3.3 and −4.7 kcal/mol, respectively. In this step, the conjugation of benzene is partially broken by the C1 hydrogenation. The reduction of π bonds to σ bonds must favor the following C−C bond cleavage involved in reaction **B**. Subsequently, the isomerization of $\mathbf{A8}^{CS}$ to the stable $\mathbf{3}^{CS}$ spontaneously occurs through the appropriate rotation of the $[C_6H_7]^-$ moiety with a ΔG° value of −7.6 kcal/mol.

For reaction **B** in Scheme 1, the singlet PES is much more favorable than the triplet one with similar structures, and an EST similar to that in reaction **A** was observed here. The most favorable PES is described in Figure 3 (see Figures S8 and S10 for the triplet and CS singlet PESs, respectively). Optimized structures for selected important stationary points are shown in Figure 4 (see Figure S9 for the whole set of optimized structures). The conversion from $\mathbf{3}^{CS}$ to $\mathbf{2}^{CS}$ consists of three fundamental steps: (i) oxidative addition ($\mathbf{3}^{CS} \rightarrow \mathbf{B2}^{CS}$), (ii) hydride−proton exchange ($\mathbf{B2}^{CS} \rightarrow \mathbf{B8}^{CS}$), and (iii) reductive elimination ($\mathbf{B8}^{CS} \rightarrow \mathbf{2}^{CS}$). The oxidative addition of the C1(sp^3)−C6(sp^2) bond to the Ti2(II) center can be understood by the charge transfer (CT) from the Ti2 $3d_\pi$ orbital to the low-lying empty σ^*_{C1-C6} antibonding orbital.[19] This CT stabilizes transition state $\mathbf{TS8}^{CS}$ and promotes the C1−C6 bond cleavage and dual Ti2−C bond formations. The population changes of the trinuclear titanium moiety are consistent with the CT discussed above (see Figure S12). This step affords the high-energy Ti(II)−Ti(IV)−Ti(IV) intermediate $\mathbf{B1}^{CS}$, with a $\Delta G^{\circ\ddagger}$ value of 21.8 kcal/mol. Subsequently, the stable intermediate $\mathbf{B2}^{CS}$ is spontaneously obtained from $\mathbf{B1}^{CS}$ with a small $\Delta G^{\circ\ddagger}$ value of 2.4 kcal/mol.

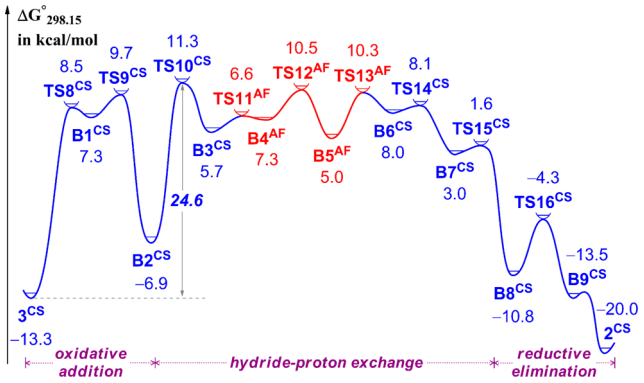

Figure 3. Singlet Gibbs energy profile ($\Delta G^{\circ}_{298.15}$) of reaction **B** in Scheme 1.

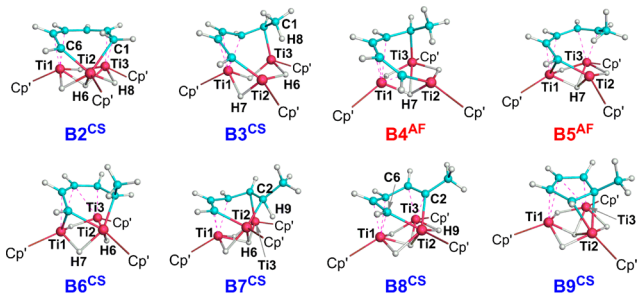

Figure 4. Optimized structures for selected important stationary points in the PES of Figure 3.

DOI: 10.1021/jacs.6b02433
J. Am. Chem. Soc. 2016, 138, 11069−11072

The rate-determing hydride−proton exchange occurs via an inter-HT ($\mathbf{B2}^{CS} \rightarrow \mathbf{B3}^{CS}$), intramolecular isomerizations ($\mathbf{B3}^{CS} \rightarrow \mathbf{B7}^{CS}$), and a proton transfer ($\mathbf{B7}^{CS} \rightarrow \mathbf{B8}^{CS}$). In the inter-HT, μ-H8 of the trinuclear titanium moiety migrates to C1 of the $[C_6H_7]^{3-}$ moiety through $\mathbf{TS10}^{CS}$, with a moderate $\Delta G^{\circ\ddagger}$ value of 18.2 kcal/mol. In this step, the C1−H8 bond is formed to obtain the methyl group of the $[C_6H_8]^{4-}$ moiety, and μ_3-H6 becomes μ-H6. Prior to the proton transfer, $\mathbf{B3}^{CS}$ spontaneously isomerizes to $\mathbf{B7}^{CS}$ via consecutive rearrangement of hydrides and Ti−C bonds. Furthermore, two ESTs ($\mathbf{B3}^{CS} \rightarrow \mathbf{B4}^{AF}$ and $\mathbf{B5}^{AF} \rightarrow \mathbf{B6}^{CS}$) are involved in this multistep isomerization. This process has $\Delta G^{\circ\ddagger}$ and ΔG° values of 4.8 and −2.7 kcal/mol, respectively. Then a barrier-free proton transfer occurs through $\mathbf{TS15}^{CS}$ to afford $\mathbf{B8}^{CS}$. In this step, proton H9 connected to C2 of the $[C_6H_8]^{4-}$ moiety migrates to the trinuclear titanium moiety and then becomes μ-H9 interacting with Ti2 and Ti3. Besides the above stepwise hydride−proton exchange process, a one-step intramolecular proton transfer pathway ($\mathbf{B1}^{CS} \rightarrow \mathbf{B8}^{CS}$) was also evaluated and was found to have a very large $\Delta G^{\circ\ddagger}$ value of 65.3 kcal/mol relative to $\mathbf{3}^{CS}$ (Figure S13). By comparison, the stepwise hydride−proton exchange pathway is obviously favorable with a moderate $\Delta G^{\circ\ddagger}$ value of 24.6 kcal/mol, in line with the experimental observation (23.2 kcal/mol).[9]

The last process of reaction **B** is the reductive elimination, in which the formation of the C2−C6 bond occurs through $\mathbf{TS16}^{CS}$ to afford $\mathbf{B9}^{CS}$, followed by an isomerization to give the Ti(II)−Ti(IV)−Ti(IV) complex $\mathbf{2}^{CS}$ with a $[MeC_5H_4]^{3-}$ moiety.[9] The $\Delta G^{\circ\ddagger}$ for this step is 6.5 kcal/mol.

The "two-state reactivity" mechanism fits with the reaction monitoring by ^{1}H NMR spectroscopy, which showed that $\mathbf{3}^{CS}$ was first formed and then disappeared to yield $\mathbf{2}^{CS}$.[9] The experiments reported that temperature affected the reaction progress. Reaction **A** could be achieved at 10 °C, whereas the subsequent reaction **B** took place at a higher temperature (40 °C). This is because $\Delta G^{\circ\ddagger}$ for reaction **B** is larger than that of reaction **A**.

In conclusion, the mechanistic details of the C−C bond cleavage and rearrangement of benzene by a trinuclear titanium hydride have been theoretically disclosed here. A novel "two-state reactivity" mechanism has been proposed. The spin inversion and electronic state transformation participate in this reaction and thus effectively decrease the activation barrier. Furthermore, the synergetic effect between trinuclear titanium centers and hydrides has been rationalized: the hydride transfers are responsible for reducing partial π bonds to σ bonds of benzene (reaction **A**), whereas the trinuclear titanium moiety plays a key role in the C−C σ bond activation and reformation (reaction **B**).

■ ASSOCIATED CONTENT

Supporting Information

The Supporting Information is available free of charge on the ACS Publications website at DOI: 10.1021/jacs.6b02433.

Computational details, complete ref 14, Figures S1−S13, Tables S1−S13, Scheme S1, and Cartesian coordinates of optimized structures in this work (PDF)

■ AUTHOR INFORMATION

Corresponding Authors

*guanw580@nenu.edu.cn

*zmsu@nenu.edu.cn

Notes

The authors declare no competing financial interest.

■ ACKNOWLEDGMENTS

This work was supported by the NNSFC (21403033). We are grateful to Dr. Yue Chen (Hokkaido University) for useful discussions and computational support.

■ REFERENCES

(1) (a) van der Boom, M. E.; Milstein, D. *Chem. Rev.* **2003**, *103*, 1759. (b) Chen, F.; Wang, T.; Jiao, N. *Chem. Rev.* **2014**, *114*, 8613. (c) Weires, N. A.; Baker, E. L.; Garg, N. K. *Nat. Chem.* **2016**, *8*, 75.

(2) (a) Thakur, A.; Facer, M. E.; Louie, J. *Angew. Chem., Int. Ed.* **2013**, *52*, 12161. (b) Masarwa, A.; Didier, D.; Zabrodski, T.; Schinkel, M.; Ackermann, L.; Marek, I. *Nature* **2014**, *505*, 199. (c) Chen, P. H.; Xu, T.; Dong, G. B. *Angew. Chem., Int. Ed.* **2014**, *53*, 1674. (d) Souillart, L.; Parker, E.; Cramer, N. *Angew. Chem., Int. Ed.* **2014**, *53*, 3001.

(3) Youn, S. W.; Kim, B. S.; Jagdale, A. R. *J. Am. Chem. Soc.* **2012**, *134*, 11308.

(4) (a) Dreis, A. M.; Douglas, C. J. *J. Am. Chem. Soc.* **2009**, *131*, 412. (b) Sattler, A.; Parkin, G. *Nature* **2010**, *463*, 523. (c) Li, H.; Li, Y.; Zhang, X. S.; Chen, K.; Wang, X.; Shi, Z. J. *J. Am. Chem. Soc.* **2011**, *133*, 15244.

(5) (a) Ozkal, E.; Cacherat, B.; Morandi, B. *ACS Catal.* **2015**, *5*, 6458. (b) Kang, Y.-W.; Cho, Y. J.; Ko, K.-Y.; Jang, H.-Y. *Catal. Sci. Technol.* **2015**, *5*, 3931.

(6) (a) Skucas, E.; MacMillan, D. W. C. *J. Am. Chem. Soc.* **2012**, *134*, 9090. (b) DiRocco, D. A.; Rovis, T. *J. Am. Chem. Soc.* **2012**, *134*, 8094. (c) Mustard, T. J. L.; Mack, D. J.; Njardarson, J. T.; Cheong, P. H. Y. *J. Am. Chem. Soc.* **2013**, *135*, 1471. (d) Krautwald, S.; Sarlah, D.; Schafroth, M. A.; Carreira, E. M. *Science* **2013**, *340*, 1065.

(7) Nishiura, M.; Hou, Z. M. *Nat. Chem.* **2010**, *2*, 257.

(8) Shima, T.; Hu, S. W.; Luo, G.; Kang, X. H.; Luo, Y.; Hou, Z. M. *Science* **2013**, *340*, 1549.

(9) Hu, S. W.; Shima, T.; Hou, Z. M. *Nature* **2014**, *512*, 413.

(10) Becke, A. D. *J. Chem. Phys.* **1993**, *98*, 5648.

(11) Lee, C.; Yang, W.; Parr, R. G. *Phys. Rev. B: Condens. Matter Mater. Phys.* **1988**, *37*, 785.

(12) Zhao, Y.; Truhlar, D. G. *Theor. Chem. Acc.* **2008**, *120*, 215.

(13) (a) Barone, V.; Cossi, M. *J. Phys. Chem. A* **1998**, *102*, 1995. (b) Cossi, M.; Rega, N.; Scalmani, G.; Barone, V. *J. Comput. Chem.* **2003**, *24*, 669. (c) Tomasi, J.; Mennucci, B.; Cammi, R. *Chem. Rev.* **2005**, *105*, 2999.

(14) Frisch, M. J.; et al. *Gaussian 09*, revision D.01; Gaussian, Inc.: Wallingford, CT, 2009.

(15) (a) Filatov, M.; Shaik, S. *J. Phys. Chem. A* **1998**, *102*, 3835. (b) Danovich, D.; Shaik, S. *J. Am. Chem. Soc.* **1997**, *119*, 1773. (c) Shaik, S.; Danovich, D.; Fiedler, A.; Schröder, D.; Schwarz, H. *Helv. Chim. Acta* **1995**, *78*, 1393.

(16) Mai, B. K.; Kim, Y. *Angew. Chem., Int. Ed.* **2015**, *54*, 3946.

(17) (a) Schröder, D.; Shaik, S.; Schwarz, H. *Acc. Chem. Res.* **2000**, *33*, 139. (b) Shaik, S.; Hirao, H.; Kumar, D. *Acc. Chem. Res.* **2007**, *40*, 532. (c) Lifshitz, C.; Gotkis, Y.; Ioffe, A.; Laskin, J.; Shaik, S. *Int. J. Mass Spectrom. Ion Processes* **1993**, *125*, R7.

(18) (a) Koga, N.; Morokuma, K. *Chem. Phys. Lett.* **1985**, *119*, 371. (b) Harvey, J. N.; Aschi, M. *Phys. Chem. Chem. Phys.* **1999**, *1*, 5555. (c) Harvey, J. N. *Phys. Chem. Chem. Phys.* **2007**, *9*, 331. (d) Harvey, J. N. *WIREs Comput. Mol. Sci.* **2014**, *4*, 1.

(19) Guan, W.; Sakaki, S.; Kurahashi, T.; Matsubara, S. *ACS Catal.* **2015**, *5*, 1.

DOI: 10.1021/jacs.6b02433
J. Am. Chem. Soc. 2016, 138, 11069−11072